

B. V. Bagryanov, G. A. Kvaskov,  
S. A. Novikov, and V. A. Sinitsyn

UDC 620.178.7

In studying the dynamic strength of structures and materials, the load is usually placed on test objects by rectangular or trapezoidal pressure pulses. In addition, their amplitude and duration vary over wide ranges. Such a loading pressure pulse can be obtained with impact loading through a special damper, for which the dependence of the force on the magnitude of compression has a region where the compression force is constant. Polystyrene foam is an example of a material used for such a damper [1, 3]. However, widespread use of polystyrene foam for these purposes is hampered by the instability of its strength characteristics, which decrease the reproducibility of test results, and comparatively low strength, which limits the level of loads that are created. In this respect, tubular crushers under axial compression have more universal possibilities.

The results of static tests of crushers, made of thin-walled aluminum tubes (the ratio of the wall thickness  $h$  to the radius of the middle surface  $R$  is less than 0.05), are presented in [4]. The results of static and dynamic tests of tubular crushers, made of polyvinyl chloride, are presented in [5]. Both types of crushers were deformed in a similar manner. The process of axial compression was accompanied by a local loss of stability with the formation of axisymmetrical and nonaxisymmetrical creases [6]. The compression force of the crusher during crease formation varied, fluctuating near some average value.

In this paper, we present the results of dynamic tests of tubular crushers, made of standard tubes (All-Union State Standard (GOST) 1947-56; AD1M, AMtsM, AMg6M, and D16T aluminum alloys). The dimensions of the crushers tested (outer diameter  $d$ , wall thickness  $h$ , length  $l$ , relative wall thickness  $h/R$ ) and some handbook characteristics of the tubes, out of which they were made (yield stress  $\sigma_{0.2}$  and breaking point  $\sigma_{bp}$ ), are presented in Table 1, where some stress characteristics of crushers, obtained while analyzing the experimental results on the dynamic compression of crushers, are also given: average compression force  $N_{av}$  of a crusher on the segment of the compression diagram without sharply manifested hardening, maximum deformation of the crusher in experiments  $\epsilon_m$ , magnitude of the relative change in the compression force on the working part of the compression diagram  $\Delta N_1/2N_{av}$ , magnitude of the relative amplitude of fluctuations in the compression force of the crusher with crease formation  $A_m/2N_{av}$ .

The crusher length  $l$  was chosen from the condition that the crushers remain stable in the large\* in the supercritical deformation range. For the crushers investigated, it was found experimentally that they do not lose stability in the large or for  $l/R \leq 8-10$ .

The deformation characteristics of crushers were determined from both the results of experiments with continuous recording of the compressive force using the measuring rod technique [7] (Fig. 1a) and the results of tests, in which the residual deformation of crushers was measured after the load was removed, while the compression force was determined by a computational method (Fig. 1b).

In the experiments, crusher 4 was deformed with an impact on its end face by a metallic plate 3, accelerated by detonating an explosive charge placed on it 1. In order to avoid splitting the impactor 3, a thin damping layer 2 was placed between it and the explosive charge. The other end face of the crusher rested either on a stationary foundation 6 or on the measuring rod 8. In loading several crushers in a single experiment, thin cardboard linings 5 were used in order to fix their mutual positioning. The deformation of the measuring rod was measured in the experiment with the help of strain gauges 7.

\*Euler form of stability loss.

TABLE 1

Number of crusher	$\varnothing d \times h \times l, 10^{-3} \text{ m}$	$h/R$	Material	$\sigma_{0.2}, 10^7 \text{ N/m}^2$	$\sigma_{bp}, 10^7 \text{ N/m}^2$	$N_{av}, 10^3 \text{ N}$	$\varepsilon_m, \%$	$\frac{\Delta N_1}{2N_{av}}$	$\frac{A_m}{2N_{av}}$
1	$\varnothing 6 \times 1 \times 20$	0,40	AD1M	—	$\leq 12$	3,0	70	0,22	—
2	$\varnothing 8 \times 1 \times 30$	0,29				3,3	70	0,08	—
3	$\varnothing 14 \times 1 \times 50$	0,15				5,0	—	—	0,28
4	$\varnothing 16 \times 2 \times 65$	0,29				12,5	55	0,20	0,08
5	$\varnothing 8 \times 1 \times 30$	0,29	Amtsm	—	$\leq 13$	4,4	70	0,07	—
6	$\varnothing 10 \times 1 \times 40$	0,22				6,2	70	0,04	—
7	$\varnothing 10 \times 2 \times 40$	0,50				Hardening			—
8	$\varnothing 13,5 \times 1,75 \times 50$	0,30	Amg6M	$\geq 15$	$\geq 32$	26,0	—	—	0,15
9	$\varnothing 14 \times 1 \times 50$	0,15				11,0	—	—	0,40
						27,5	60	0	0,40
10	$\varnothing 20 \times 1,5 \times 80$	0,16	D16T	$\geq 26$	$\geq 42$	Failure			
11	$\varnothing 10 \times 1 \times 40$	0,22							

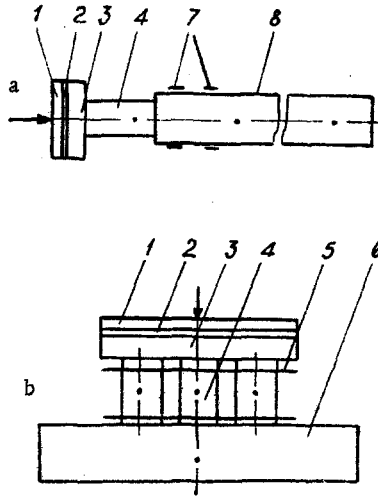


Fig. 1

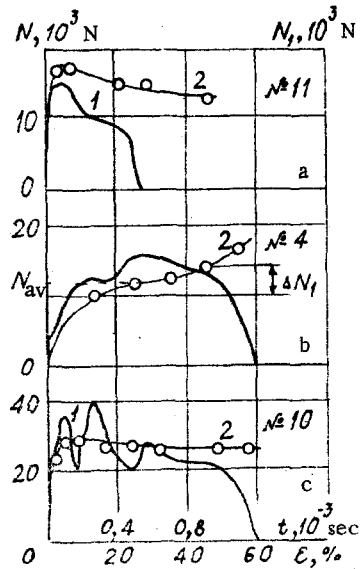


Fig. 2

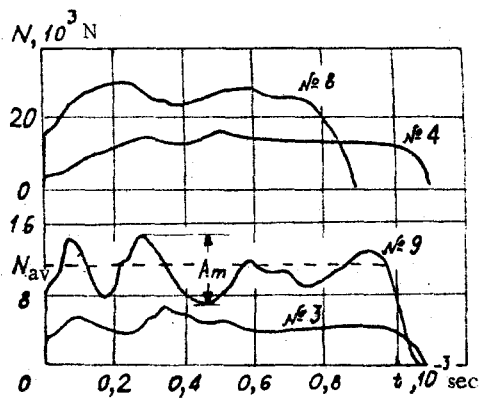


Fig. 3

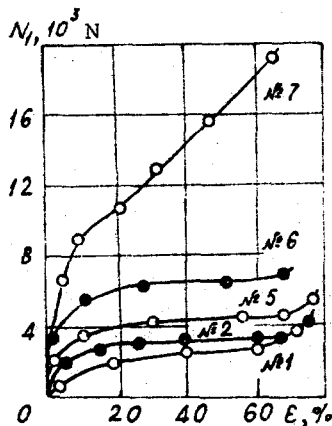


Fig. 4



Fig. 5

The compression force  $N$  obtained as a function of time  $t$  using the measuring rod technique is shown in Figs. 2 (curve 1) and 3 for different tubular crushers.

In the other method used in this work for determining the deformation properties of tubular crushers, the compression force was found by a computational method using the known kinetic energy of the impactor  $E$  (in the experiments, the velocity of the impactor was measured) and the deformation of the crushers  $\Delta l = \epsilon l$ , measured after the experiment, using the equations [3]  $N_1 = E/\epsilon l$ . In addition, two assumptions were made: All of the kinetic energy of the impactor goes into compression of the crusher; and on the segment of the compression diagram studied in each of the tests, the crushers are compressed by constant force.

By successively changing in the experiments the magnitude of the deformation of the crushers, it is possible to construct quite accurately the average (integral) compression diagram of tubular crushers  $N_1 = f(\epsilon)$  (Fig. 2, curve 2; Fig. 4). The points on the curves  $N_1 = f(\epsilon)$  correspond to maximum deformation of crushers in successive experiments. A deformed crusher is shown in Fig. 5.

It is convenient to compare different tubular crushers, as material for an impact damper, according to the following characteristics, presented in Table 1 and in Figs. 2-4 (the numbers of the crushers from the table are shown in the figures):  $\epsilon_m$ ,  $N_{av}$ ,  $\Delta N_1/2N_{av}$ ,  $A_m/2N_{av}$ .

In practice, the magnitude of the maximum deformation of the crusher on the working part of the compression diagram  $\epsilon_m$  is limited by fixing the allowable magnitude of the relative change in the compression force.

All of the characteristics of tubular crushers indicated above depend on the mechanical properties of the crusher material and on the relative thickness of its walls. The results of tests on tubular crushers made of aluminum alloys under axial dynamic compression lead to several results useful in practice.

1. The relative amplitude of the oscillations in the axial compressive force is smaller in crushers made of softer alloys. For the same crushers, compression diagrams obtained with the help of the measuring rod and computed from the maximum compression agree well (see Fig. 2b).

The relative amplitude of the oscillations in the axial compressive force for tubular crushers decreases with increasing relative wall thickness (see Fig. 3).

3. For crushers with a wall thickness  $h/R > 0.4$ , there is an appreciable increase in the compressive force (hardening) with increasing deformation (Fig. 4, crusher 7).

4. For crushers with wall thickness  $h/R < 0.3$ , there are two forms of local stability loss: first, an axisymmetrical ring-shaped crease forms on the end face opposite the one bearing the load; then, rhombiform creases form (Fig. 5a). For crushers with  $h/R > 0.3$ , only ring-shaped creases form (Fig. 5b). For crushers made of quenched D16T alloy, during deformation ( $\epsilon > 20\%$ ), the wall cracks along the generatrix and the compression force decreases (Fig. 2a).

#### LITERATURE CITED

1. Yu. V. Bat'kov, S. I. Bodrenko, et al., "Explosive method of calibrating piezoelectric accelerometers using porous dampers," in: Reports at the First All-Union Symposium on Pulsed Pressures [in Russian], Vol. 1, VNIIFTRI, Moscow (1974).
2. B. I. Abashkin, I. Kh. Zabiroy, and V. G. Rusin, "Dynamic compressibility of polystyrene foam," Mekh. Polim., No. 1 (1977).
3. Yu. A. Krysanov and S. A. Novikov, Investigation of the dynamic compression of polystyrene foam," Zh. Prikl. Mekh. Tekh. Fiz., No. 8 (1977).
4. A. Pugsley and M. Macaulay, "The large-scale crumpling of thin cylindrical columns," Q. J. Mech. Appl. Math., 13, Pt. 1 (1960).
5. P. D. Soden and S. T. S. Al-Hassani, and W. Johnson, "The crumpling of polyvinyl chloride tubes under static and dynamic axial loads," Inst. Phys. Conf. Ser., No. 21 (1974).
6. A. S. Vol'mir, Stability of Elastic Systems [in Russian], Fizmatgiz, Moscow (1963).
7. G. Kol'skii, Investigation of Mechanical Properties of Materials under High Loading Rates," Mekhanika, No. 4 (1950).